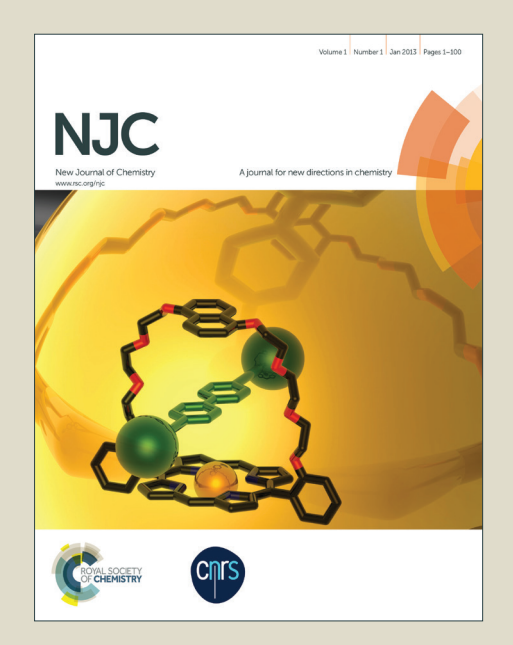
NJC

Accepted Manuscript



This is an *Accepted Manuscript*, which has been through the Royal Society of Chemistry peer review process and has been accepted for publication.

Accepted Manuscripts are published online shortly after acceptance, before technical editing, formatting and proof reading. Using this free service, authors can make their results available to the community, in citable form, before we publish the edited article. We will replace this Accepted Manuscript with the edited and formatted Advance Article as soon as it is available.

You can find more information about *Accepted Manuscripts* in the **Information for Authors**.

Please note that technical editing may introduce minor changes to the text and/or graphics, which may alter content. The journal's standard <u>Terms & Conditions</u> and the <u>Ethical guidelines</u> still apply. In no event shall the Royal Society of Chemistry be held responsible for any errors or omissions in this *Accepted Manuscript* or any consequences arising from the use of any information it contains.



1	3D sandwich-type prostate specific antigen (PSA)
2	immunosensor based on rGO-MWCNT-Pd nanocomposite
3	Lihui Tian, Lei Liu, Yueyuan Li, Qin Wei, Wei Cao *
4	Key Laboratory of Chemical Sensing & Analysis in Universities of Shandong,
5	School of Chemistry and Chemical Engineering, University of Jinan, Jinan 250022,
6	PR China
7	Corresponding author: Prof. W. Cao
8	Email address: jn_chm302@163.com (jncw88@163.com)
9	Tel.: +86-531-82767890.
10	Fax: +86-531-82765475.
11	

Abstract

1

2

3

4

5

6

7

8

9

10

11

12

13

14

15

16

17

18

19

20

21

In this work, a novel and ultrasensitive sandwich-type electrochemical immunosensor was developed for the quantitative detection of prostate specific antigen (PSA), a well-known prostatic tumor biomarker. 3D-structured reduced graphene oxide - multiwalled carbon nanotube - palladium nanoparticles (NPs) nanocomposite (rGO-MWCNT-Pd) is prepared by a simple and environmentally way and utilized for the adsorption of the secondary antibodies (Ab₂). It is used as novel enzyme-mimetic label to develop of the sandwich-type electrochemical immunosensor for signal amplification, showing better electrocatalytic activity towards the reduction of hydrogen peroxide (H₂O₂) than rGO-CNT or rGO-Pd due to the synergetic effect presented in rGO-MWCNT-Pd nanocomposite. Au NPs decorated amination of graphene (Au-NH₂-GS) nanocomposite is used as platform for immobilization of primary antibobies (Ab₁) via amide reaction between -NH₂ group in Au-NH₂-GS and -COOH groups in Ab₁. Due to the excellent electrocatalytic activity of rGO-MWCNT-Pd towards the reduction of (H₂O₂), electrochemical amperometric changes to different concertrations of PSA are achieved after the immunoreaction. Under the optimum experimental conditions, the proposed electrochemical sandwich-type immunosensor exhibits a low detection limit (0.17 pg/mL), a wide linear range (from 0.5 pg/mL to 15 ng/mL) for the detection of PSA. And it shows high sensitivity, good selectivity and stability, holding a great potential in clinical and diagnostic applications.

- 1 Keywords: Prostate specific antigen; 3D structured; rGO-MWCNT-Pd nanocomposite;
- 2 Sandwich-type immunosensor.

1 Introduction

1

2

3

4

5

6

7

8

9

10

11

12

13

14

15

16

17

18

19

20

21

22

Prostate specific antigen (PSA) is a kind of serine protease which is produced by normal and malignant prostate epithelial cells. There will be very little PSA in the blood of a healthy man, but the levels of PSA can be increased rapidly in the blood of the patient with prostatic cancer.² PSA is the best serum marker for the detection of prostatic carcinoma.^{3, 4} At present, more than 4 ng/mL of PSA in serum, people can be considered pathologic, and when it exceeds 10 ng/mL people will be recommended as a patient with prostate cancer.⁵ So it is necessary to provide a simple, reliable and robust technique for the diagnosis of prostate cancer with detecting the content of PSA. There are many immune detection methods to detect the content of PSA, such as eneyme immunoassay and chemiluminescence immunoassays.^{6, 7} Compared with those methods electrochemical immunosensors have gained great deal of attention in recent decades, especially in clinical diagnostics, ^{8,9} due to their promising properties of sensitivity, low-cost, fast analysis, inexpensive instrumentation, suitable miniaturization, specific and simple detection. 10-12 Electrochemical immunosensors based on the specific binding of antibody-antigen are widely used to diagnose disease. 13 And sandwich-type immunosensor is one of most important immunosensors, which is primary composed of primary antibobies (Ab₁), the secondary antibodies (Ab₂) and antigen. ¹⁴ But the label-free immunoassay could not amplify the response signals and the sensitivities, detection limit of these immunosensors which need to be improved.¹⁵ In order to achieve the more effective immunosensors, we use Au

- nanoparticles (NPs) decorated amination of graphene (Au-NH₂-GS) nanocomposite as
- 2 the sensor platform to combine more antibodies and 3D-structured reduced graphene
- 3 oxide multiwalled carbon nanotube palladium nanoparticles nanocomposite
- 4 (rGO-MWCNT-Pd) as the labels of Ab₂ to amplify the response signals. With the
- 5 Au-NH₂-GS/Ab₁ capturing antigen onto the antibody site by the specific bond of the
- antigen-antibody, the rGO-MWCNT-Pd nanocomposite which is used to label Ab₂
- 7 could be successively conjugated with the antigen via the immunoreacton.

9

10

11

12

13

14

15

16

17

18

19

20

21

22

Graphene oxide (GO) is a kind of 2D structure material with large surface area. ¹⁶ In fact, most of graphene-based composites were prepared from GO. ¹⁷ GO can be converted into conductive reduced graphene oxide (rGO). However, these advantages of rGO, such as large specific surface area, high electrical conductivity, ¹⁸⁻²⁰ have been partially exploited due to the agglomeration of graphene sheets. ²⁰ In this work, we use multiwalled carbon nanotubes (MWCNTs) to solve this problem. In the past decades, too much attention has been paid on MWCNTs, ²¹ due to the exceptional mechanical properties of MWCNTs and their specific surface area. ^{22,23} The specific surface of MWCNTs is several orders of magnitude larger than conventional microfillers. ²⁴ In the study, MWCNTs are added to inhibit the polymerization of rGO during the

In recent years, noble metal NPs are widely used as electrode materials due to their superior electrocatalytic to the reduction of H₂O₂, ^{25, 26} such as Pd, Au, Ag, Pt NPs

structured rGO-MWCNT considerably larger than rGO.

process of synthesizing rGO from GO. As a result, the surface area of the 3D

- and their composite with metal oxide which have been extensively used in bioaffinity
- 2 sensors.²⁷ When the H₂O₂ is added into the bottom of the liquid, noble metal NPs can
- 3 catalyze the hydrolysis of H₂O₂, accelerate the redox reaction in the electroactive
- 4 substance, and enhance the electrochemical signal.²⁸ In this work, Pd NPs are
- 5 introduced via adding K₂PdCl₄ aqueous solution to the 3D-structured rGO-MWCNT
- 6 nanocomposite in an ice bath.²⁹ The special structure of rGO-MWCNT
- 7 nanocomposite with large surface area provides more active sites for Pd NPs to
- 8 catalyze the hydrolysis of H₂O₂. As the superior electrocatalytic to the reduction of
- 9 H₂O₂ of Pd NPs, the electrocatalytic of the immunosensor is obviously increased.
- The immobilization of Ab₁ is also important for the sensitivity of the
- immunosensor.³⁰ In this work, Au@NH₂-GS with good electron transfer ability,
- biocompatibility and large specific surface area is used as platform for immobilization
- of Ab_1 , which enhances the loading of antiboby.

2 Materials and methods

14

15

2.1 Apparatus and reagents

- All electrochemical measurements were performed on a CHI760D
- 17 electrochemical workstation (Huakeputian Technology Beijing Co., Ltd., China).
- 18 Transmission electron microscope (TEM) images were obtained from a Hitachi H-600
- 19 microscope (Japan). Scanning electron microscope (SEM) images and energy
- 20 dispersive X-ray spectral data (EDX) were obtained using Quanta FEG250 field
- emission environmental SEM (FEI, United States) operated at 4KV.
- 22 PSA and anti-PSA were purchased from Biocell Company (Zhengzhou, China).

- Bovine serum albumin (BSA 96-99%) was purchased from Sigma. MWCNTs were
- 2 purchased from Timesnano. Phosphate buffered saline (PBS) was used as an
- 3 electrolyte for all electrochemistry measurement. All other reagents were of analytical
- 4 grade and ultrapure water was used throughout the study.

5 **2.2 Preparation of the Au@NH₂-GS**

- In this process, GO was synthesized by the modified Hummers method.³¹ The
- 7 NH₂-GS was synthesized with the following method. 0.1 g of GO was dispersed to 10
- 8 mL of absolute ethyl alcohol in a flask with ultrasonically stirring for 1h. After further
- 9 addition of 0.2 mL of (3-Aminopropyl) triethoxysilane (99 wt%) for reaction, under
- 10 70 °C and stirred for 1.5 h. Then, hydrazine hydrate (0.1 mL, 80 wt%) was added in
- the above solution, under 90°C for 1 h. After that the solution was centrifuged (9000
- 12 rpm for 20 min). Then NH₂-GS was obtained at 40 °C for 12 h. Au NPs were
- synthesized by the classical Frens method. In brief, a solution of HAuCl₄ (0.01 wt%,
- 14 100 mL) was heated to boiling, and then a solution of trisodium citrate (1 wt%, 2.5
- 15 mL) was added. The boiling solution turned a brilliant ruby-red in around 15 min,
- indicating the formation of monodisperse spherical particles, and then it was cooled to
- 17 room temperature.

21

- 18 15 mg of NH₂-GS was mixed with 15 mL of the prepared Au NPs solution under
- 19 stirring for 12 h, and then Au@NH2-GS nanocomposite was obtained by
- 20 centrifugation and dried at vacuum.

2.3 Preparation of the rGO-MWCNT-Pd@Ab₂

30 mg of MWCNTs were mixed with 30 mL 2 mg/mL of homogeneous GO

- aqueous dispersion, then the mixture was sonicated for 30 min. After that, it was
- sealed in a 50 mL of Teflon-lined autoclave at 180 °C for 12 h, then cooled in room
- 3 temperature. The rGO-MWCNT nanocomposite was obtained after freeze-dried
- 4 overnight. Then 1 mL of K₂PdCl₄ (10 mM) aqueous solution and 5 mg of
- 5 rGO-MWCNT nanocomposite was added into a 10 mL of aqueous solution under
- 6 vigorous stirring for 30 min in an ice bath. Afterwards, the products were washed
- 7 three times with ultrapure water and centrifuged to remove the remaining reagents.
- 8 Then the rGO-MWCNT-Pd nanocomposite was obtained under the condition of
- 9 vacuum at 40 °C for 12 h.
- Fig.1 (A) shows the illustration of fabrication procedure of the
- 11 rGO-MWCNT-Pd@Ab₂. 2 mL of rGO-MWCNT-Pd (3 mg/mL) solution was added to
- 12 100 μL Ab₂ dispersion (10 μg/mL) and the mixture was tirred for 12 h at 4 °C
- following centrifugation. The rGO-MWCNT-Pd@Ab₂ was dispersed in 2 mL of PBS
- (pH=7.4) and stored at 4 °C.

17

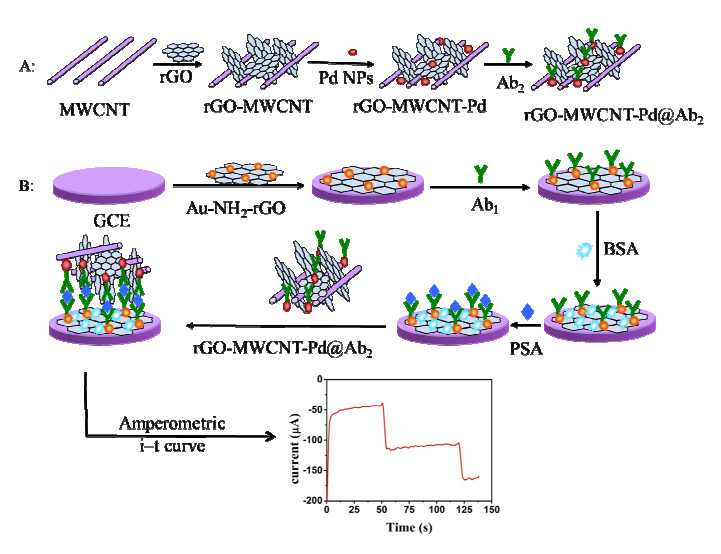


Fig.1. (A) The illustration of fabrication procedure of the rGO-MWCNT -Pd@Ab₂. (B) The illustration of fabrication procedure of the immunosensor.

2.4 Fabrication of the immunosensor

Fig.1 (B) shows the illustration of fabrication procedure of the immunosensor. A glassy carbon electrode (GCE) was polished to a mirror-like finish with alumina powder, after cleaned before using by ultrapure water. First, 6 μL of prepared Au-NH₂-GS solution was added onto the electrode surface via physical adsorption and then dried. After washing 6 μL Ab₁ (10 μg/mL) was added onto the electrode surface and after dried at 4 °C the electrode was washed carfully. Then, 3 μL of BSA (1 wt%) solution was added to eliminate nonspecific binding sites. Following that, the electrode was washed and incubated with a varying concentration of PSA at 4 °C. Then the electrode was washed by ultrapure water to remove unbounded PSA molecules. Finally, the prepared rGO-MWCNT-Pd@Ab₂ buffer solution was added onto the electrode surface at 4 °C, and the electrode was washed thoroughly for measurement.

2.5 Detection of PSA

A conventional three-electrode system was used for all electrochemical measurements: a GCE with 4 mm in diameter as the working electrode, a saturated calomel electrode (SCE) as the reference electrode, and a platinum wire electrode as the counter electrode. The PBS at pH=7.4 was used for all the electrochemical measurements. When the background current was stabilized, 5 mM H₂O₂ was added into the PBS. A detection potential of -0.4 V was selected in amperometric *i*–*t* curve technology which was used to record the amperometric change.

3 Results and discussion

1

7

- 2 In this section, we conducted a series of characterizations for the nanocomposites
- of Au@NH₂-GS and rGO-MWCNT. Then we optimized the experimental conditions.
- 4 Under the optimal conditions, we obtained the equation of the calibration curve for
- 5 detection of PSA. After all of that, the proposed immunosensor was applied to detect
- 6 PSA in the serum.

3.1 Characterization of the Au@NH2-GS and rGO-MWCNT-Pd

Fig.2 (A) shows the SEM image of the Au@NH₂-GS. There are some 8 9 corrugations on the edge of the NH₂-GS, which is consistent with previous work. 10 From the image we can see a large number of Au NPs were successfully attached and well distributed onto the surface of the NH₂-GS. Although the obtained Au NPs have 11 12 high surface energy, they can not move free and aggregate further, by the interaction between Au NPs and -NH₂. In order to better distinguish the surface structure of the 13 14 MWCNTs and the rGO-MWCNT nanocomposite, the morphology of those were 15 characterized through SEM (Fig. 2 B and C). From Fig. 2(B), the structure of untreated 16 carbon nanotubes are thin long tubular, stacked between multiple tubes winding form a mesh structure without any impurities. But the external structure of the 17 18 rGO-MWCNT is completely different with it. As can be seen from the picture of (C), 19 hierarchical tortuous MWCNTs interspersed into the rGO sheets, and rGO likes a layer of gauze covering on the surface of the MWCNTs. MWCNTs can bridge the 20 21 adjacent rGO sheets, prevent rGO sheets from restacking, and increase the specific surface area. The 3D structured rGO-MWCNT nanocomposite provides more active 22

- sites for Pd NPs. As the superior electrocatalytic to the reduction of H₂O₂ of Pd NPs,
- 2 the electrocatalytic of the immunosensor was increased obviously. Fig.2 (D) is the
- 3 TEM image of rGO-MWCNT-Pd nanocomposite. Pd NPs can be seen clearly, and it
- 4 can be further confirmed the special structure of rGO-MWCNT-Pd nanocomposite.
- 5 Fig.2 (E) shows the EDX spectrum of the prepared rGO-MWCNT-Pd nanocomposite.
- 6 Pd element in the EDX spectrum proofs that the preparation of the composite
- 7 materials was very successful.

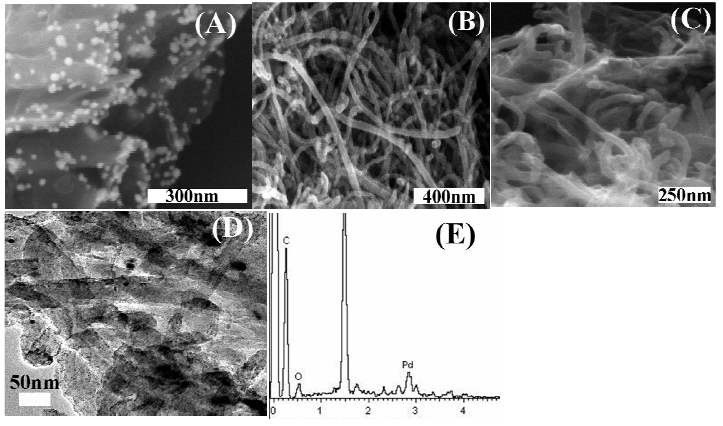


Fig.2. (A) The SEM image of Au@NH₂-GS; (B) MWCNTs; (C) rGO-MWCNT; (D) The TEM image of rGO-MWCNT-Pd nanocomposite; (E) EDX spectrum of rGO-MWCNT-Pd nanocomposite

10 11

12

13

14

15

16

17

18

19

3.2 Optimization of experimental conditions

In order to obtain the optimal electrochemical signal, we select the best experimental conditions including pH, the concentration of Au@NH₂-GS and rGO-MWCNT-Pd. These conditions on the experimental are very important for the detection of PSA. The immunosensor is tested by amperometric *i*–*t* curve in the working solution of PBS. Fig.3 (A) shows the amperometric changes in different pH values of PBS. As shown, from 4.5 to 7.4 of pH the amperometric change is increased, and then from 7.4 to 9.2 it is decreased. The best amperometric change is achieved at

- pH=7.4. This proves that the pH values have a significant impact on the redox
- 2 procedure of H₂O₂. The highly acidic or alkaline surroundings would damage antigen
- and antibody so that the electrochemical behavior of the immunosensor will become
- 4 bad.

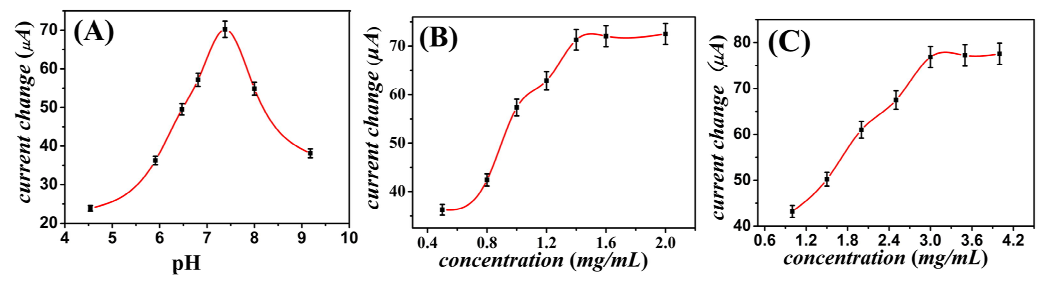


Fig.3. (A) Amperometric changes of the immunosensor of 1 ng/mL PSA to the reduction of 5 mM H_2O_2 in different pH values of PBS (B) Au@N H_2 -GS concentration and (C) rGO-MWCNT-Pd@Ab₂ concentration. Error bar = RSD (n = 5)

The role of Au@NH₂-GS is to capture more antibodys with little resistance increasement, so the influence of Au@NH₂-GS concentration can not be ignored. Fig.3 (B) shows the amperometric changes when the immunosensor is modified with different concentrations of Au@NH₂-GS. The amperometric change is increased from 0.5 to 1.4 mg/mL, after that it reaches a plateau. Au@NH₂-GS have good electrical conductivity may be attributed to the increase of specific surface area and electroactive materials. While too much Au@NH₂-GS may not be increase the electrical conductivity. In our work, we used 1.4 mg/mL of Au@NH₂-GS to conduct the electrochemical tests.

rGO-MWCNT-Pd is used as the lable of Ab₂, so the concentration of rGO-MWCNT-Pd is also important for the electrochemical tests. When the immunosensor was modified with different concentrations of rGO-MWCNT-Pd@Ab₂, the result of amperometric change is shown in Fig.3 (C). From 1.0 to 3.0 mg/mL the

- 1 amperometric change is increased and then reaches a plateau. The more
- 2 rGO-MWCNT-Pd, the more Ab₂ would be captured. But a certain amount of
- 3 Au@NH₂-GS@Ab₁ could only combined with a certain number of antigen, so
- 4 over-much rGO-MWCNT-Pd is wasted. In our study, we used 3.0 mg/mL of
- 5 rGO-MWCNT-Pd to capture Ab₂ more efficient.

6 3.3 Characterization of the immunosensor

hydrolysis of H₂O₂.

20

7 In our study, amperometric i-t curve technology is used to explore the electrocatalytic performance of rGO-MWCNT-Pd nanocomposite. The results of the 8 9 study are shown in Fig.4 (A). These curves respectively represent bare GCE (a); the 10 immunosensor for the detection of 1 ng/mL PSA modified without lables (b); with rGO-Pd@Ab₂ (c) and rGO-MWCNT-Pd@Ab₂(d) as lables. As seen from Fig.4 (A), 11 12 the curves of (a) and (b) are almost the straigh lines, in other words, the bare GCE and the immunosensor modified without lables have no effect on the redox procedure of 13 14 H₂O₂. Comparing with curve (a) and curve (b), curve (c) displays lager amperometric change. It indirect proof Pd NPs have a great catalytic activity for H₂O₂. As 15 expected, the immunosensor using rGO-MWCNT-Pd as label displayed the highest 16 current change (curve d), that is because rGO-MWCNT could combine more Pd NPs. 17 18 It further evidence that the 3D structured of rGO-MWCNT nanocomposite has large 19 surface area and it could provides more active sites for Pd NPs to catalyze the

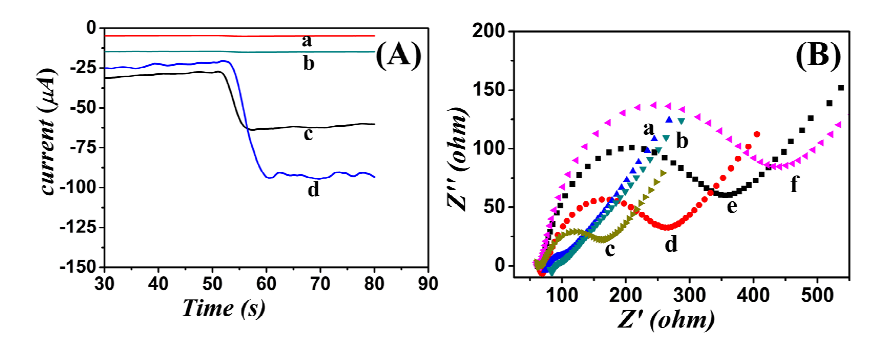


Fig.4. (A) Amperometric changes of the immunosensor for the detection of 1 ng/mL PSA without lables (b), with rGO-Pd@Ab₂ (c) and rGO-MWCNT-Pd@Ab₂(d) as lables, the bare GCE (a). (B) Nyquist plots of the AC impedance for each immobilized step of bare GCE (a), Au@NH₂-GS/GCE (b), Au@NH₂-GS@Ab₁/GCE (c) BSA/Au@NH₂-GS@Ab₁/GCE (d) PSA/BSA/Au@NH₂-GS@Ab₁/GCE (e) and rGO-MWCNT-Pd@Ab₂/PSA/BSA /Au@NH₂-GS@Ab₁/GCE (f) in 0.1 M KCl and 2.5 mM Fe(CN)₆⁴⁻/Fe(CN)₆⁴⁻.

10

11

12

13

14

15

16

17

18

19

20

21

22

1 2

3

4

5

6

In this study, the assembly process of the electrode was characterized by the AC impedance tecnology. Fig.4 (B) shows the Nyquist plots of A.C. impedance spectroscopy in the process of modifying electrode. Nyquist plots comprise; two parts the linear portion and the semicircle portion. The linear portion at low frequencies is affiliated with electrochemical behavior limited by diffusion. The semicircle portion at high frequencies is affiliated with the electrochemical process subject to electron transfer, and the greater resistance, the greater diameter. Thus, it is an appropriate tecnology to observe the changes of resistance in the surface of the electrode. In this Au@NH2-GS/GCE Au@NH2-GS@Ab1/GCE study, (b), (c) $BSA/Au@NH_2-GS@Ab_1/GCE$ (d) $PSA/BSA/Au@NH_2-GS@Ab_1/GCE$ (e) rGO-MWCNT-Pd@Ab₂/PSA/BSA /Au@NH₂ -GS@Ab₁/GCE (f) were modified layer by layer on the bare GCE (a). The increased diameter indicated that the resistance is increasing gradually. Based on the result of this study, we conclude that the electron transfer ability of the modified electrode is determined by the conductive

- 1 nanocomposite and non-conductive bioactive substances. Clearly, the assembly of
- these materials and biomolecules onto the surface of the electrode was successful.
- In this study, the sandwich-type electrochemical immunosensor was used to
- 4 detect different concentrations of PSA under the optimal experimental conditions.
- 5 Fig.5 shows the amperometric changes increase linearly with the logarithmic values
- of the PSA concentration, within the range from 0.5 pg/mL to 15 ng/mL, and with a
- low limit of 0.17 pg/mL. The equation of the calibration curve is $\Delta I = 11.83 \text{ lgC} + 11.83 \text{ lgC}$
- 8 77.42, r=0.9913. The low detection limit owed to the several reasons. Firstly,
- 9 Au-NH₂-GS with good biocompatibility could capture more Ab₁ to amplify the signal.
- Secondly, the 3D stetured of rGO-MWCNT-Pd nanocomposite has large specific
- surface area, excellent electrocatalytic activity and biocompatibility, which could
- greatly increasing the response to H_2O_2 , and broaden the scope of testing and leading
- to higher sensitivity.

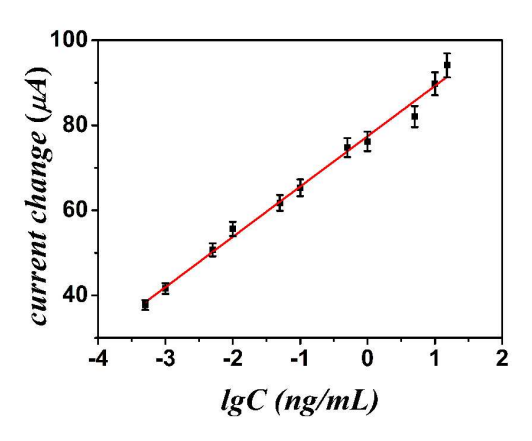


Fig. 5. Calibration curve of the immunosensor to logarithmic values of the PSA concentrations. Error bar = RSD (n = 5)

16

17

18

19

3.4 Reproducibility, stability and selectivity of the immunosensor

In this work, a series of five immunosensors were prepared for the detection of 1 ng/mL PSA to testify the reproducibility of the immunosensor. Fig.6 shows that the

- relative standard deviation (RSD) of the measurements is 2.51%. It can be proved
- 2 that the reproducibility of the prepared immunosensor are quite good.³²

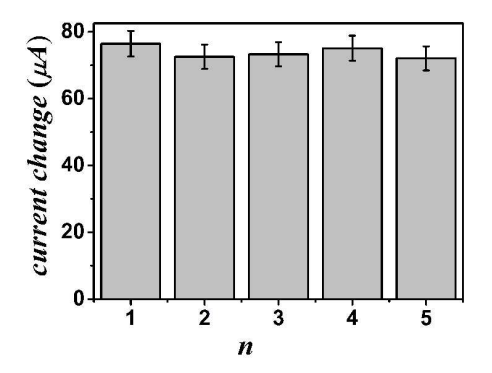


Fig.6. Amperometric changes of biosensor to five immunosensors treated in same situation.

In order to test the stability of the immunosensor, the sensor was stored at 4 °C

- 6 for two weeks, which not in use. There was not significant reduction compared with
- 7 the immunosensors without being stored. This could owe to the biocompatibility of
- 8 the rGO-MWCNT-Pd nanocomposite and large specific surface area Au@NH2-GS
- 9 nanocomposite.

5

11

12

14

15

17

To test the selectivity of the immunosensor, interferences study was performed

using vitamin C, carcinoembryonic antigen (CEA), glucose and alpha fetal protein

(AFP). The concentrations of the interferences were 100 ng/mL. These four

substances changed the current values less than 5.0 % of that without interferences.

It can be concluded that the reproducibility, stability and selectivity of the

immunosensor are acceptable, and the proposed immunosensor can be used to detect

the PSA.

3.5 Real sample analysis

From above of all, the proposed immunosensor can be used in the detection of the PSA. In order to prove this, the proposed immunosensor was used to detect the

- amount of PSA in the serum, and then the recovery test was carried out to prove the
- 2 results. The results of the experimental are showed in Table 1. We can see that the
- RSD is in the range from 3.89 % to 4.75 % and the recovery is in the range from
- 4 96.0 % to 98.0%. So the proposed immunosensor can be used to detect the PSA in
- 5 human serum.

Table 1Determination of PSA in human serum sample

Initial PSA concentration in sample (ng/mL)	Added PSA concentration (ng/mL)	Measured concentration after addition (ng/mL)	Average value (ng/mL)	RSD (%,n=5)	Recovery $(\%, n = 5)$
0.98	1	1.86, 1.92, 2.05, 1.97, 2.02	1.96	3.89	98.0
	2	2.81, 2.95, 3.11, 2.76, 2.86	2.90	4.75	96.0
	3	4.12, 3.81, 3.76, 3.79, 4.05	3.91	4.30	97.7

4 Conclusion

In this work, a sandwich-type immunosensor based on 3D-structured reduced graphene oxide - multiwalled carbon nanotube - palladium nanoparticles nanocomposite as labels for the quantitative detection of prostate specific antigen is development. The existence of multiwalled carbon nanotubes inhibit the polymerization of rGO during the process of synthesizing rGO from GO. They also increase the surface area of the nanocomposite and provide more active sites for Pd nanoparticles to catalyze the hydrolysis of H₂O₂. As a result, the electrocatalytic of the immunosensor is obviously increased. The 3D sandwich-type immunosensor is successfully developed within a wide range (0.5 pg/mL~15 ng/mL) and a low detection limit (0.17 pg/mL^{*}). This result is better than many other electrochemical

- 1 methods, as shown in Table 2.³³⁻³⁶ Besides, the proposed immunosensor also showed
- 2 good reproducibility, high selectivity and acceptable stability. Generally speaking, the
- 3 3D-structured immunosensor can provide wide potential applications for the detection
- 4 of PSA in clinical diagnosis.

5 Table 2

6 Comparing with other immunoassay biosensing system

	<u>.</u>			
Detection	Biomarker	Linear range	Detection limit	References
methods	protein	(ng/mL)	(pg/mL)	
electrochemical	PSA	0.005-10	2	33
electrochemical	PSA	0.01-40	2	34
electrochemical	PSA	0.0048-0.1168	0.0016	35
electrochemical	PSA	0.01-10	2	36
electrochemical	PSA	0.0005-15	0.0017	Proposed method

7

8

Acknowledgments

- 9 This work was supported by the Natural Science Foundation of Shandong
- 10 Province (No. ZR2011BL008), the Natural Science Foundation of China (Nos.
- 11 21175057 and 21377046).

References

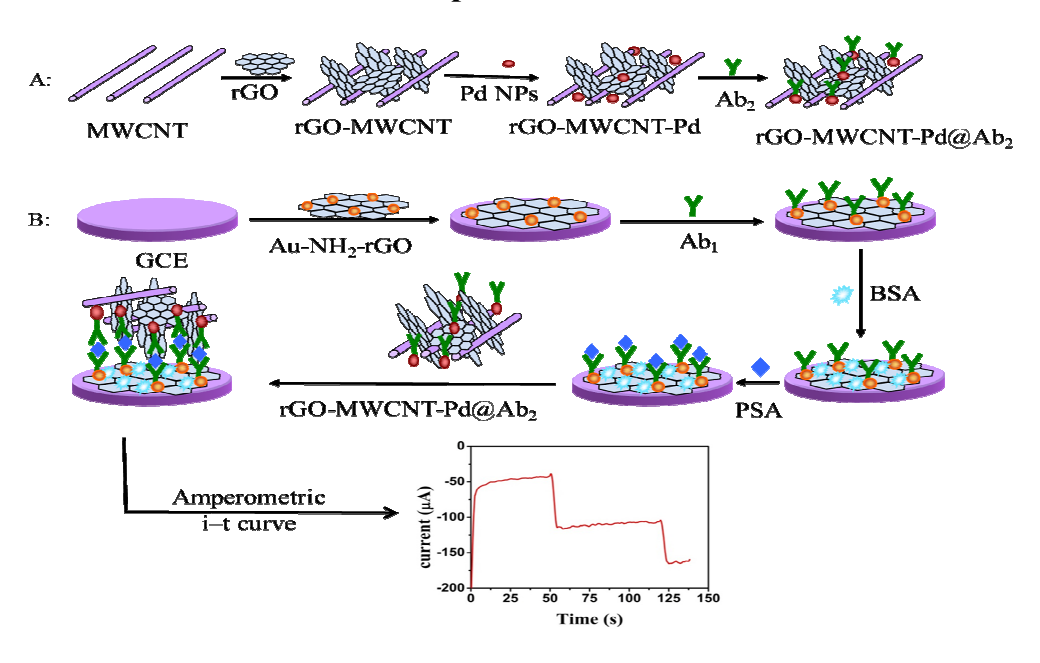
- 2 1. S. P. Balk, Y. J. Ko, G. J. Bubley, Journal of Clinical Oncology, 2003, 21,
- 3 383-391.
- 4 2. S. W. Lee, K. Hosokawa, S. Kim, T. Laurell, M. Maeda,, Sensing and
- 5 Bio-Sensing Research, 2015, 3, 105-111.
- 6 3. D. A. Healy, C. J. Hayes, P. Leonard, L. Mckenna, R. O'Kennedy, Trends in
- 7 Biotechnology, 2007, 25, 125-131.
- 8 4. F. H. Schröder, J. Hugosson, M. J. Roobol, T. L. Tammela, S. Ciatto, V. Nelen, M.
- 9 Kwiatkowski, M. Lujan, H. Lilja, M. Zappa, New England Journal of Medicine,
- 10 2009, 360, 1320-1328.
- 5. M. Bo, M. Ventura, R. Marinello, S. Capello, G. Casetta, F. Fabris, Critical
- Reviews in Oncology Hematology, 2003, 47, 207-211.
- 13 6. H. Adel Ahmed, H. M. Azzazy, Biosensors and Bioelectronics, 2013, 49,
- 14 478-484.
- 15 7. R. Liu, C. Wang, Q. Jiang, W. Zhang, Z. Yue, G. Liu, Analytica Chimica Acta,
- 16 2013, 801, 91-96.
- 17 8. Y. Cai, H. Li, Y. Li, Y. Zhao, H. Ma, B. Zhu, C. Xu, Q. Wei, D. Wu, B. Du,
- Biosensors and Bioelectronics, 2012, 36, 6-11.
- 19 9. R. Feng, Y. Zhang, H. Ma, D. Wu, H. Fan, H. Wang, H. Li, B. Du, Q. Wei,
- 20 Electrochimica Acta, 2013, 97, 105-111.
- 21 10. P. K. Vabbina, A. Kaushik, N. Pokhrel, S. Bhansali, N. Pala, Biosensors and

- 1 Bioelectronics, 2015, 63, 124-130.
- 2 11. Z. Dai, F. Yan, H. Yu, X. Hu, H. Ju, Journal of Immunological Methods, 2004,
- 3 287, 13-20.
- 4 12. N. Li, Y. Wang, Y. Li, W. Cao, H. Ma, D. Wu, B. Du, Q. Wei, Sensors and
- 5 Actuators B: Chemical, 2014, 202, 67-73.
- 6 13. J. H. Jung, D. S. Cheon, F. Liu, K. B. Lee, T. S. Seo, Angewandte Chemie
- 7 International Edition, 2010, 49, 5708-5711.
- 8 14. Y. Z. Wu, N. Gan, F. T. Hu, T. H. LI, Y. T. CAO, L. Zheng, Chinese Journal of
- 9 Analytical Chemistry, 2011, 39, 1634-1640.
- 10 15. P. Yang, X. Li, L. Wang, Q. Wu, Z. Chen, X. Lin, Journal of Electroanalytical
- 11 Chemistry, 2014, 732, 38-45.
- 12 16. J. H. Kim, S. Lee, J. W. Lee, T. Song, U. Paik, Electrochimica Acta, 2014, 125,
- 13 536-542.
- 14 17. S. Chandrasekaran, W. M. Choi, J. S. Chung, S. H. Hur, E. J. Kim, Materials
- 15 Letters, 2014, 136, 118-121.
- 16 18. J. Xia, F. Chen, J. Li, N. Tao, Nature Nanotechnology, 2009, 4, 505-509.
- 19. Y. Zhu, S. Murali, M. D. Stoller, K. Ganesh, W. Cai, P. J. Ferreira, A. Pirkle, R.
- 18 M. Wallace, K. A. Cychosz, M. Thommes, Science, 2011, 332, 1537-1541.
- 19 20. M. F. El-Kady, V. Strong, S. Dubin, R. B. Kaner, Science, 2012, 335, 1326-1330.
- 20 21. D. Weidt, Ł. Figiel, Computational Materials Science, 2014, 82, 298-309.
- 21 22. C. Cooper, R. Young, M. Halsall, Composites Part A: Applied Science and
- 22 Manufacturing, 2001, 32, 401-411.

- 1 23. I. Diaconu, C. Cristea, V. Hârceagă, G. Marrazza, I. Berindan-Neagoe, R.
- 2 Săndulescu, Clinica Chimica Acta, 2013, 425, 128-138.
- 3 24. A. Peigney, C. Laurent, E. Flahaut, R. Bacsa, A. Rousset, Carbon, 2001, 39,
- 4 507-514.
- 5 25. F. Meng, X. Yan, J. Liu, J. Gu, Z. Zou, Electrochimica Acta, 2011, 56,
- 6 4657-4662.
- 7 26. E. Kurowska, A. Brzózka, M. Jarosz, G. Sulka, M. Jaskuła, Electrochimica Acta,
- 8 2013, 104, 439-447.
- 9 27. X. Luo, A. Morrin, A. J. Killard, M. R. Smyth, Electroanalysis, 2006, 18,
- 10 319-326.
- 11 28. F. Liu, G. Xiang, X. Chen, F. Luo, D. Jiang, S. Huang, Y. Li, X. Pu, RSC
- 12 Advances, 2014, 4, 13934-13940.
- 13 29. T. Sun, Z. Zhang, J. Xiao, C. Chen, F. Xiao, S. Wang, Y. Liu, Scientific Reports,
- 14 2013, 3**,** 2527.
- 15 30. Y. Wang, Y. Zhang, Y. Su, F. Li, H. Ma, H. Li, B. Du, Q. Wei, Talanta, 2014, 124,
- 16 60-66.
- 17 31. D. C. Marcano, D. V. Kosynkin, J. M. Berlin, A. Sinitskii, Z. Sun, A. Slesarev, L.
- B. Alemany, W. Lu, J. M. Tour, ACS Nano, 2010, 4, 4806-4814.
- 19 32. R. Feng, Y. Zhang, H. Yu, D. Wu, H. Ma, B. Zhu, C. Xu, H. Li, B. Du, Q. Wei,
- Biosensors and Bioelectronics, 2013, 42, 367-372.
- 21 33. Q. Wei, T. Li, G. Wang, H. Li, Z. Qian, M. Yang, Biomaterials, 2010,
- 22 31,7332-7339.

- 1 34. H. Li, Q. Wei, J. He, T. Li, Y. Zhao, Y. Cai, B. Du, Z. Qian, M. Yang, Biosensors
- and Bioelectronics, 2011, 26, 3590-3595.
- 3 35. N. Xia, D. Deng, L. Zhuang, B. Yuan, M. Jing, J. Du, L. Liu, Biosensors and
- 4 Bioelectronics, 2013, 43, 155-159.
- 5 36. Y. Li, J. Han, R. Chen, X. Ren, Q. Wei, Analytical Biochemistry, 2015,
- 6 469,76-82.

Graphical Abstract



The signal amplification sandwich-stype immunosensor with wide linear range and low detection limit in clinical and diagnostic applications.

 Table 1

 Determination of PSA in human serum sample

Initial PSA concentration in sample (ng/mL)	Added PSA concentration (ng/mL)	Measured concentration after addition (ng/mL)	Average value (ng/mL)	RSD (%,n=5)	Recovery $(\%, n = 5)$
	1	1.86, 1.92, 2.05,	1.96	3.89	98.0
0.98		1.97, 2.02			
	2	2.81, 2.95, 3.11,	2.90	4.75	96.0
		2.76, 2.86			
	3	4.12, 3.81, 3.76,	3.91	4.30	97.7
		3.79, 4.05			

 Table 2

 Comparing with other immunoassay biosensing system

Detection methods	Biomarker protein	Linear range (ng/mL)	Detection limit (pg/mL)	References
electrochemical	PSA	0.005-10	2	33
electrochemical	PSA	0.01-40	2	34
electrochemical	PSA	0.0048-0.1168	0.0016	35
electrochemical	PSA	0.01-10	2	36
electrochemical	PSA	0.0005-15	0.0017	Proposed method